Fuzzy Logic Control for Wind Energy Conversion System based on DFIG

Bouchaib Rached
Laboratory of Signal Analysis and Information Processing
FST Settat
Morocco
bouchaib.rached@gmail.com

Mustapha Elharoussi
Laboratory of Signal Analysis and Information Processing
FST Settat
Morocco
m.elharoussi@gmail.com

Elhassane Abdelmounim
Laboratory of Signal Analysis and Information Processing
FST Settat
Morocco
hassan.abdelmounim@hotmail.fr

***Abstract*—This paper concentrates on fuzzy logic control (FLC) of variable speed wind turbines with doubly fed induction generator(DFIG). The wind energy conversion system (WECS) is equipped with a wind turbine, a mechanical transmission system, a DFIG, a Rotor Side converter (RSC), a Grid Side converter (GSC), and a common DC-link capacitor.**

The main objective is to regulate the active power by extracting the maximum of power and to have a null stator reactive power.

In this study, four FLC are implemented separately in RSC, GSC, DC bus voltage, and the maximum power point tracking (MPPT).

The performances of the proposed controllers have been tested and compared with a PI controller.

The obtained results show a satisfactory performance in terms of stability, precision, and robustness under variable wind speed conditions.

Keywords: FLC; Vector control; WECS; DFIG; MPPT.

I. INTRODUCTION

In the last few years there has been a growing interest in renewal energy resources and their penetration into the power supply grid. Indeed, a considerable attention has been paid to wind energy generation.

Currently, the wind system using a DFIG is the more used for production of the electric energy[1][2].

WECS includes a wind turbine, a mechanical transmission system, a DFIG, and a partial scale power electronic converter.

Power electronic converter includes two main parts connected by a DC-link capacitor; RSC which feeds rotor circuit and GSC that rectifies grid voltage.

Our work consists of modelling of the chain of conversion of the wind energy where the DFIG operates at variable speed. Thereafter, we consider the regulating of powers in order to ensure an optimum operation.

Different structures and algorithms strategy can be used for control of power converters. In this article, a Mamdani fuzzy logic controller [3] is applied to control separately the RSC ,GSC, and the MPPT.

FLC doesn't require the knowledge of the exact model, it has the advantage to be robust and simple to design [3][4].

We implement this command strategy in order to meet the following specifications: Good static precision in order to obtain optimal energy production and a unit power factor; Good rejection of disturbances that can be frequent on such a system; Robustness to any parametric variations of the system.

The paper is organized as follows: in Section II, the whole association including the turbine and DFIG is modeled. In Section III, a fuzzy logic controller is developed to control separately the RSC, DC link, and the GSC. Also an MPPT strategy is designed. The obtained results are illustrated in section IV.

II. MODELING OF THE WIND POWER SYSTEM

A general scheme of WECS is shown in Fig. 1.

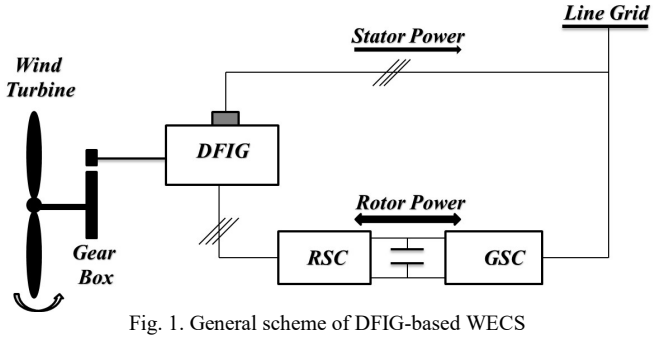

Fig. 1. General scheme of DFIG-based WECS

A. Wind turbine

The mechanical power extracted from the wind can be expressed as follows [1][2]:

$$P_{aero} = \frac{1}{2} \cdot C_P(\beta,\lambda) \cdot \rho \cdot \pi \cdot R_{Pale}^2 \cdot V_{wind}^3 \quad (1)$$

Where ρ is the air density (kg/ m³), R_{Pale} is the blade radius (m), V_{wind} is the wind speed, $C_P(\beta,\lambda)$ is the turbine power coefficient, and λ is the tip speed ratio, which is defined by:

$$\lambda = \frac{\Omega_t \cdot R_{Pale}}{V_{wind}} \quad (2)$$

Where Ω_t is the Rotational speed of the turbine.

The equation of aerodynamic torque:

$$T_{aero} = \frac{P_{aero}}{\Omega_t} = \frac{1}{2} \cdot C_P(\lambda,\beta) \cdot \rho \cdot S \cdot \frac{V_{wind}^3}{\Omega_t} \quad (3)$$

Where S is the area swept by the pales of the turbine.

The gearbox model [1][5][6]:

978-1-5386-7850-3/19/$31.00 ©2019 IEEE

$$N_G = \frac{\Omega_m}{\Omega_t} \tag{4}$$

$$T_m = \frac{T_{aero}}{N_G} \tag{5}$$

Where T_m is the mechanical torque on the rotor shaft of the generator.

The dynamic of the wind turbine is given by:

$$J \cdot \dot{\Omega}_m = T_m - K \cdot \Omega_m - T_{em} \tag{6}$$

J : the total inertia brought back to the rotor shaft of the generator;

K : Coefficient of Total Friction Returned to the Generator Rotor Shaft (Nm/rd/s).

B. DFIG model

The DFIG dynamic model is given by [7][8][9]:

Electrical equations

$$\begin{cases} V_{Sd} = R_S I_{Sd} + \frac{d}{dt}\Phi_{Sd} - \omega_S \Phi_{Sq} \\ V_{Sq} = R_S I_{Sq} + \frac{d}{dt}\Phi_{Sq} + \omega_S \Phi_{Sd} \\ V_{rd} = R_r I_{rd} + \frac{d}{dt}\Phi_{rd} - \omega_r \Phi_{rq} \\ V_{rq} = R_r I_{rq} + \frac{d}{dt}\Phi_{rq} + \omega_r \Phi_{rd} \end{cases} \tag{7}$$

Stator and rotor flux equations

$$\begin{cases} \Phi_{Sd} = L_S I_{Sd} + M I_{rd} \\ \Phi_{Sq} = L_S I_{Sq} + M I_{rq} \\ \Phi_{rd} = L_r I_{rd} + M I_{Sd} \\ \Phi_{rq} = L_r I_{rq} + M I_{sq} \end{cases} \tag{8}$$

Stator and rotor powers

$$\begin{cases} P_S = v_{Sd} \cdot i_{Sd} + v_{Sq} \cdot i_{Sq} \\ Q_s = v_{Sq} \cdot i_{Sd} - v_{Sd} \cdot i_{Sq} \end{cases} \tag{9}$$

$$\begin{cases} P_r = v_{rd} \cdot i_{rd} + v_{rq} \cdot i_{rq} \\ Q_r = v_{rq} \cdot i_{rd} - v_{rd} \cdot i_{rq} \end{cases} \tag{10}$$

The electromagnetic torque

$$T_{em} = pM\left(I_{rd} I_{Sq} - I_{rq} I_{Sd}\right) \tag{11}$$

III. FUZZY CONTROL OF WECS

A. Vector control of DFIG–RSC

We use the two-phase modeling of the machine. The reference frame (d-q) is oriented to align the axis d with the stator flux ϕ_S [10] [11] [12]:

$$\phi_{Sq} = 0 \Leftrightarrow \phi_S = \phi_{Sd} \tag{12}$$

$$\begin{cases} V_{Sd} = 0 \\ V_{Sq} = \omega_S \Phi_{Sd} = V_s \end{cases} \tag{13}$$

So, we can write:

$$\begin{cases} \Phi_{Sd} = L_S I_{Sd} + M I_{rd} \\ \Phi_{Sq} = L_S I_{Sq} + M I_{rq} = 0 \end{cases} \tag{14}$$

The adaptation of the relations (9), (10), and (14) to the chosen system of axes and the simplifying hypothesis considered in our case gives:

$$\begin{cases} P_S = -V_S \frac{M}{L_S} I_{rq} \\ Q_S = \frac{V_S \Phi_S}{L_S} - \frac{V_S M}{L_S} I_{rd} \end{cases} \tag{15}$$

$$\begin{cases} P_r = g V_S \frac{M}{L_S} I_{rq} \\ Q_r = g \frac{V_S M}{L_S} I_{rd} \end{cases} \tag{16}$$

Therefore, power control is achieved by regulating the d and q rotor currents:

$$\begin{cases} v_{rd} = R_r I_{rd} - L_r \omega_r \sigma I_{rq} + L_r \sigma \frac{dI_{rd}}{dt} \\ v_{rq} = R_r I_{rq} + L_r \omega_r \sigma I_{rd} + \frac{M \omega_r}{L_S} \Phi_{sd} + L_r \sigma \frac{dI_{rq}}{dt} \end{cases} \tag{17}$$

The plant for the current control loops is given in (18) and (19):

$$F(s) = \frac{I_{rd}(s)}{V_{rd}^r(s)} = \frac{I_{rq}(s)}{V_{rq}^r(s)} = \frac{V_S M}{R_r L_s + s L_s L_r \sigma} \tag{18}$$

$$\begin{cases} e_d = g \omega_s \frac{M}{L_S} \phi_s \\ e_q = \frac{V_S R_r}{\omega_s M} \end{cases} \tag{19}$$

Where F is the process model.

V_{rd}^r, V_{rq}^r and e_d, e_q are the controller output voltages and the compensation voltages respectively.

The FLC structure for the RSC is shown in fig. 2.

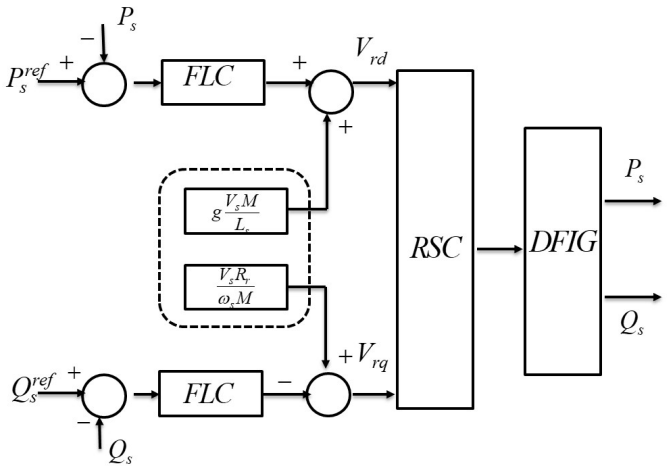

Fig.2. FLC structure for the RSC

B. Vector control of DFIG–GSC

The GSC voltages in its d-q components are obtained by the typical configuration of control strategy is given by:

$$\begin{cases} \dfrac{dI_{gd}}{dt} = -\dfrac{V_{gd}}{L} - \dfrac{R}{L} I_{gd} + \omega_s I_{gq} + + \dfrac{V_{sd}}{L} \\ \dfrac{dI_{gq}}{dt} = -\dfrac{V_{gq}}{L} - \dfrac{R}{L} I_{gq} - \omega_s I_{gd} + \dfrac{V_{sq}}{L} \end{cases} \quad (20)$$

Applying the Laplace transforms to the above two equations:

$$\begin{cases} V_{sd} = (R + sL) I_{gd} - \omega_s L I_{gq} + V_{gd} \\ V_{sq} = (R + sL) I_{gq} + \omega_s L I_{gd} + V_{gq} \end{cases} \quad (21)$$

Considering

$$\begin{cases} V_d = (R + sL) I_{gd} \\ V_q = (R + sL) I_{gq} \end{cases} \quad (22)$$

The plant for the current control loops is given by:

$$F(s) = \frac{I_{gq}}{V_q} = \frac{I_{gq}}{V_q} = \frac{1}{R + sL} \quad (23)$$

I_{gd} and I_{gq} demand being derived respectively from the DC-link voltage error through a FLC and the displacement factor on the supply side of the inductor.

Substituting (23) in (22), the reference direct and quadrature control signals can be given as:

$$\begin{cases} V_d^{ref} = -V_d + \omega_s L I_{gq} + V_{sd} \\ V_q^{ref} = -V_q - \omega_s L I_{gd} + V_{sq} \end{cases} \quad (24)$$

The FLC structure for the RSC is shown in fig. 3.

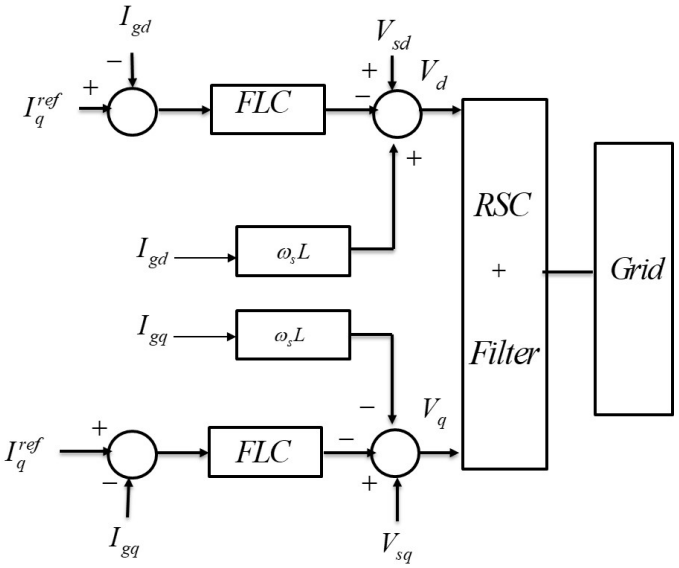

Fig.3. FLC structure for the GSC

C. DC bus voltage control

To control the DC bus voltage V_C, a regulator must be implemented to maintain this voltage constant regardless of the current flow rate on the capacitor.

the DC bus equation can be written as follows [13]:

$$P_c = c v_c \frac{dv_c}{dt} = P_g - P_r \quad (25)$$

Where P_r and P_g are the active power at RSC and GSC side, respectively.

To control the V_C, we control the P_c in the capacitor by adjusting the power P_g.

The structure of FLC for DC-link voltage is shown at fig.4.

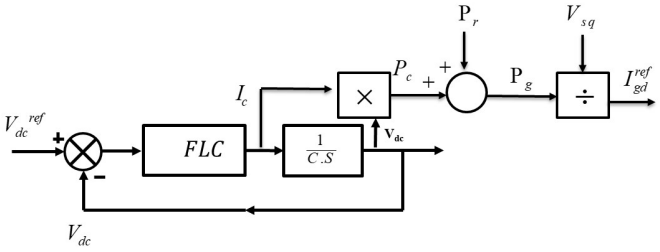

Fig.4. FLC for DC-link voltage

D. MPPT strategy

The objective of this section is to develop an MPPT strategy for optimal energy transfer in DFIG-based wind energy systems.

Maximum power point tracking (MPPT) can be realized in the RSC control by adjusting the power command [14].

C_p must be maintained at its maximum in order to reach the T_{opt}, which is given by the following equation:

$$T_{opt} = k_{opt} \cdot \Omega_m^{\,2} \quad (26)$$

Where, $$K_{opt} = \frac{1}{2} \cdot \rho \cdot \pi \cdot R_{Pâle}^{5} \cdot \frac{C_{PMAX}}{\lambda^{3}_{opt}} \quad (27)$$

The figure 5 shows the proposed control structure:

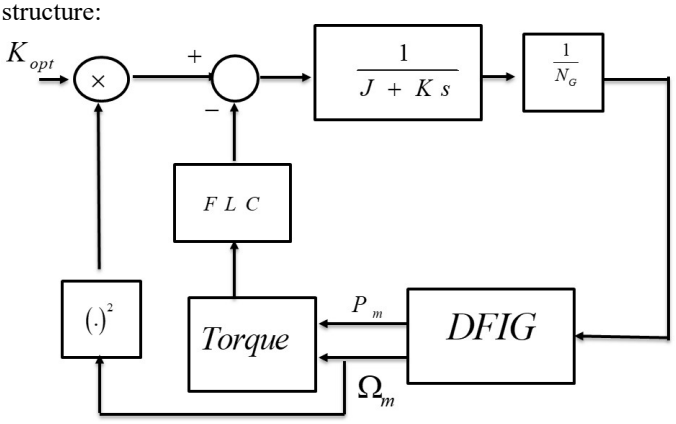

Figure 5: MPPT based on FLC

E. *Fuzzy Logic Controller*

Fuzzy controller uses a systematic method to control a nonlinear procedure based on human experience. This is defined as heuristic method this can enhance the operation of closed loop system. The operation of the fuzzy controller is based on its capability to simulate several role implications at the same time procedure, and it results the significantly comprehensive output[3][4][15].

The fuzzy control based on Mamdani model is presented in fig.6. [3][4][15].

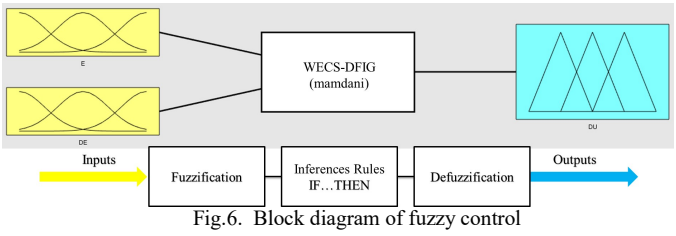

Fig.6. Block diagram of fuzzy control

Fuzzy controller inputs are the error and its derivative, while the output is the command itself. Triangular and trapezoidal membership functions are used on a universe of discourse normalized in the range [-1; 1] for the inputs (error (E), error variation (DE)) and output (input process) as shown in fig.7.

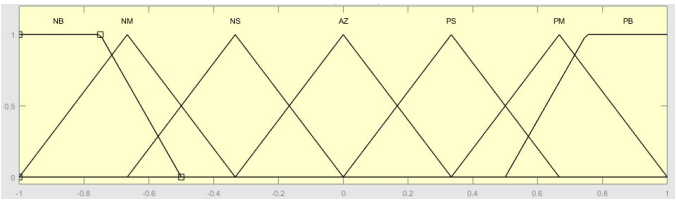

Fig.7. Membership functions of inputs and outputs

The fuzzy sets are defined as follows:

NB: Negative-Big; NM: Negative-Medium; NS: Negative-Small; AZ: About-Zero; PS: Positive-Small; NM: Positive-Medium; PB: Positive-Big.

The fuzzy rules, for determining output variable of the controller as a function of input variables are grouped in the Table 1.

Table1 Rule matrix for fuzzy logic controllers

DE \ E	NB	NM	NS	AZ	PS	PM	PB
NB	NB	NB	NB	NB	NM	NS	AZ
NM	NB	NB	NB	NM	NS	AZ	PS
NS	NB	NB	NM	NS	AZ	PS	PM
AZ	NB	NM	NS	AZ	PS	PM	PB
PS	NM	NS	AZ	PS	PM	PB	PB
PM	NS	AZ	PS	PM	PB	PB	PB
PB	AZ	PS	PM	PB	PB	PB	PB

IV. SIMULATION RESULTS

The proposed FLC model is implemented in MATLAB/Simulink. The parameters of WECS for a simulation [16] are presented in table 3.

The speed of the generator is depicted in figure 8.

Figures 9 and 10 show the waveform of the currents.

Figure 11 presents the stator power and its reference profiles resulting of the MPPT and injected into the grid.

In order to test the robustness of the controllers, the following test condition is used:

Variation in rotor resistance: t = 12 [s], Rr →2* Rr.

Figure 12, shows the effect of this variation on the active power response for fuzzy logic controllers.

As illustrate at figures 13 and 14, the two components Irq and Ird are evolving as expected since decoupling works fine.

As illustrate at figure 15, a good response of DC-link voltage is achieved.

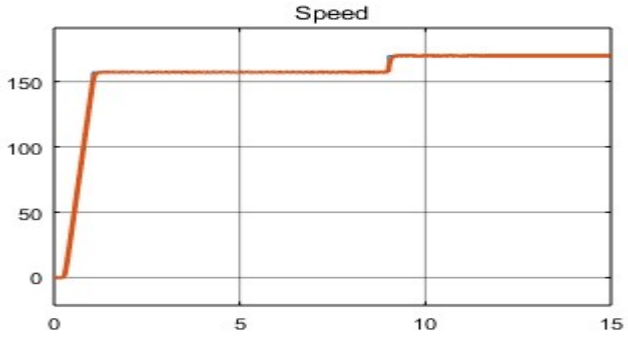

Fig. 8. Speed response

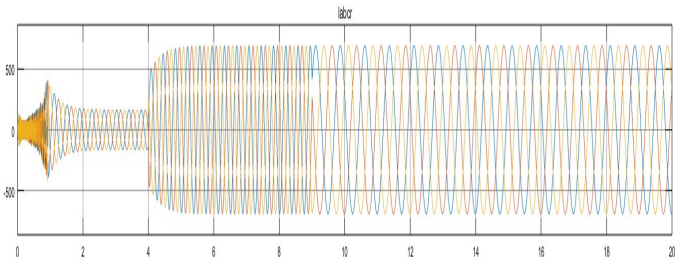

Fig. 9. Rotor current response

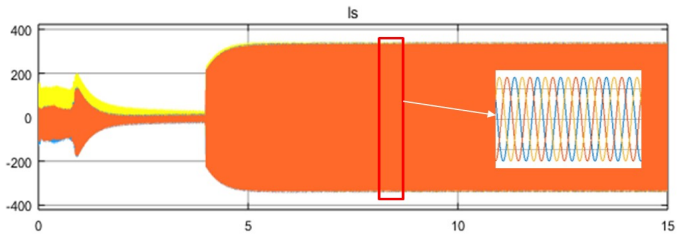

Fig. 10. Stator current response

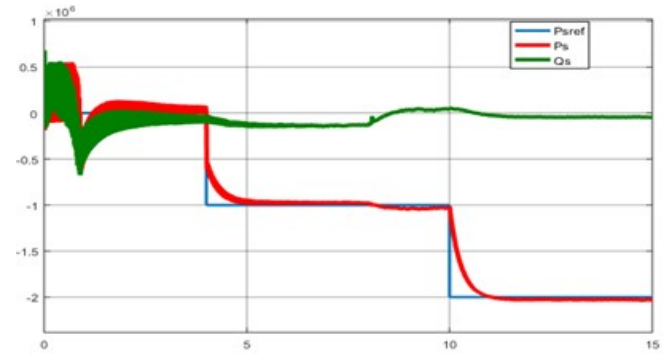

Fig. 11. Stator power response

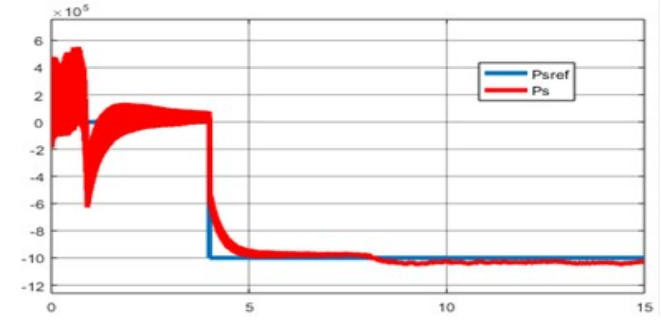

Fig. 12. Stator active power response during variations of Rr

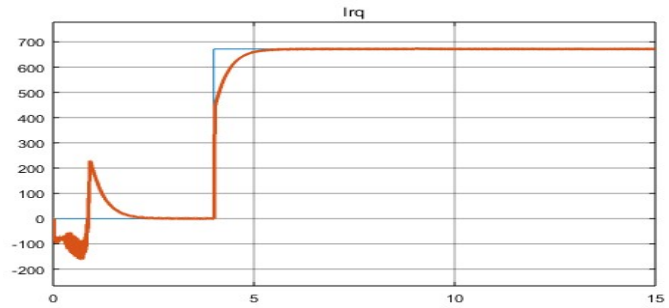

Fig. 13. Quadrature rotor current response

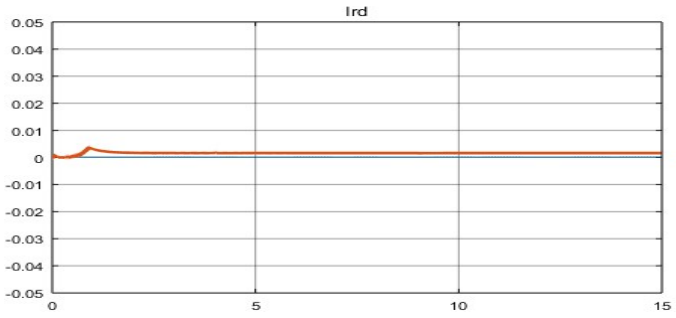

Fig. 14. Direct rotor current response

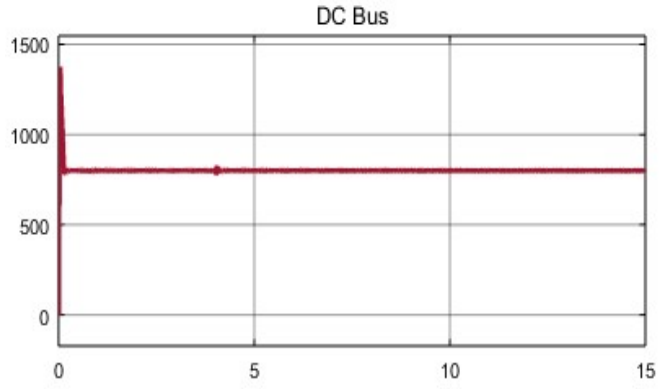

Fig. 15. DC-link voltage response

In order to validate the performance of FLC and to compare the obtained results with other controllers, we implemented a PI controller in our platform.

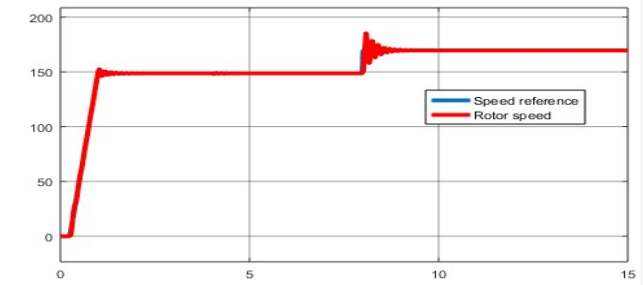

Fig. 16. Speed response (PI)

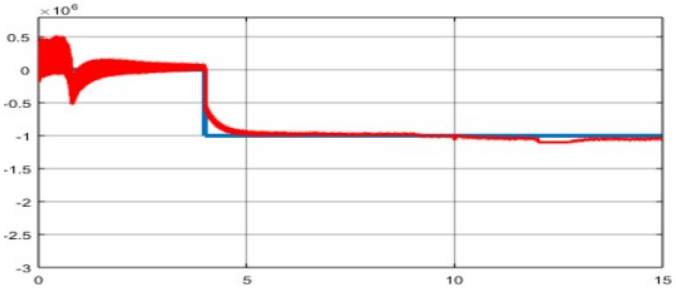

Fig. 17. Stator power response during variations of Rr (PI)

According to figures 16 and 17, which show the results of the implementation of PI controllers on wind power systems, and by observing the previous results, we see that the behaviour of two controllers (PI controller and FLC) are identical during continuous regimes, but the fuzzy controller has a clear advantage:

-Fewer oscillations at start-up and during setpoint changes;

-The peaks of disturbances are much less significant with the FLC in particular.

The comparison results are summarized in the following table:

Table2 Behavior of PI controllers and FLC

	oscillations	**Parameters variations**
FLC	Less significant	No influence
PI	Quite significant	the time response is altered

V. CONCLUSION

In this paper a design of an optimal fuzzy logic controller for wind turbine on 1.5 MW DFIG application is presented.

At first, a model of the turbine and the generator are proposed. Then, a control strategy based on fuzzy logic allowing independent control of the converters and the MPPT has been presented.

Summing up the results, it can be concluded that the measured powers follow perfectly their references and with perfect decoupling between the two axes d and q at steady state. The obtained performances are no overshoot, no static error, rather fast response time, and robustness.

APPENDIX

Table 3 Detailed parameters of the DFIG

Blade Radius R	35.25 m
Rs	0.012Ω
Rr	0.021Ω
Ls	0.0137 H
Lr	0.0136 H
M	0.0135H
J	0.175 kg.m²
K	0.0024 N/rd/s
p	2
R	0.4 Ω
L	3 mH
C	2.2 mF

REFERENCES

[1] I. Munteanu, Optimal control of wind energy systems : towards a global approach. Springer, 2008.

[2] G. Abad, Doubly fed induction machine : modeling and control for wind energy generation applications. Wiley-Blackwell Pub, 2011.

[3] J. Trivedi and T. Agarwal, "Controlling and Analysis of Variable Wind Speed Turbine with DFIG Using Fuzzy Logic Controller," vol. 12, no. 5, pp. 21–28, 2017.

[4] Hong Hee Lee, Phan Quoc Dzung, Le Minh Phuong, Le Dinh Khoa, and Nguyen Huu Nhan, "A new fuzzy logic approach for control system of wind turbine with Doubly Fed Induction Generator," in International Forum on Strategic Technology 2010, pp. 134–139, 2010.

[5] P. M. M. Bongers, "Modeling and Identification of Flexible Wind Turbines and A Factorizational Approach to Robust Control Design." PhD thesis, Delft University of Technology, June 94.

[6] B. Beltran et al., "A combined high gain observer and high-order sliding mode controller for a DFIG-based wind turbine," in Proceedings of the IEEE ENERGYCON'10, Manama (Bahraïn), pp. 322-327, December 2010.

[7] G. S. Kaloi, J. Wang, and M. H. Baloch, "Active and reactive power control of the doubly fed induction generator based on wind energy conversion system," Energy Reports, vol. 2, pp. 194–200, Nov. 2016.

[8] C. Hamon, K. Elkington, and M. Ghandhari, "Doubly-fed induction generator modeling and control in DigSilent PowerFactory," International Conference on Power System Technology, pp. 1–7, 2010.

[9] A. Boyette, "Contrôle-commande d'un générateur asynchrone à double alimentation avec système de stockage pour la production éolienne," Thèse de doctorat en génie électrique, Université Henri Poincaré, Nancy I, 11, France, 2006.

[10] S. Khojet El Khil, I. Slama-Belkhodja, M. Pietrzak-David, and B. de Fornel, "Power distribution law in a Doubly Fed Induction Machine," Math. Comput. Simul., vol. 71, no. 4–6, pp. 360–368, Jun. 2006.

[11] E. Lotfi, B. Rached, M. Elhaissouf, M. Elharoussi, and E. Abdelmounim, "DSP implementation in the loop of the vector control drive of a permanent magnet synchronous machine," in ACM International Conference Proceeding Series, 2017, pp. 1–7.

[12] M. Elhaissouf, E. Lotfi, B. Rached, M. Elharoussi, and A. Barazzouk, "DSP Implementation in the Loop of the Indirect Rotor Field Orientation control for the Three-Phase Asynchronous Machine," in Proceedings of the 2nd International Conference on Computing and Wireless Communication Systems - ICCWCS'17, 2017, pp. 1–7.

[13] L. Fan and Z. Miao, Modeling and analysis of doubly fed induction generator wind energy systems. Academic Press, 2015.

[14] A. E. H. A. A. De Adel Abdelbaset, Yehia S. Mohamed, Abou-Hashema M. El-Sayed, Wind Driven Doubly Fed Induction Generator: Grid Synchronization and Control - Adel Abdelbaset, Yehia S. Mohamed, Abou-Hashema M. El-Sayed, Alaa Eldin Hussein Abozeid Ahmed - Google Livres. 2010.

[15] A. Dida and D. Benattous, "A complete modeling and simulation of DFIG based wind turbine system using fuzzy logic control," Front. Energy, vol. 10, no. 2, pp. 143–154, Jun. 2016.

[16] S. El Aimani, Intégration des éoliennes dans les réseaux électriques Modélisation et commande de technologies. Presses Académiques Francophones, 2012.